Marie Skłodowska-Curie Actions (MSCA)
Innovative Training Networks (ITN)
H2020-MSCA-ITN-2019

861079 – NextMGT

(Next Generation of Micro Gas Turbines for High Efficiency, Low Emissions and Fuel Flexibility)

Technological advances in electrical and electronic parts and control system

Deliverable No. 19
D3.3

Date: 26 June 2022

This project has received funding from the European Union's Horizon 2020 research and innovation programme under Marie Sklodowska-Curie grant agreement No 861079

Contents

List of Figures

Nomenclature

MGT	*Micro Gas Turbine*
CHP	*Combined Heat and Power*
GHG	*Green House Gas*
CCP	*Combined Cooling and Power*
CCHP	*Combined Cooling Heating and Power*
NG	*Natural Gas*
ESR	*Early-Stage Researcher*
EIA	*Energy Information Administration*
EU	*European Union*
FEL	*Following Electrical Load*
FTL	*Following Thermal Load*
HD	*Heat Driven*
ED	*Electrical Driven*
BL	*Base Load*
FHL	*Following Hybrid Load*
PEC	*Power Energy Consumption*
CDE	*Carbon Dioxide Emissions*
PGU	*Power Generation Unit*
GSHP	*Ground Source Heat Pump*
ATC	*Annual Total Cost*
HETS	*Hybrid Electrical-Thermal Strategy*
ES	*Emission Strategy*
ICE	*Internal Combustion Engine*
FGR	*Flue Gas Reinjection*
TIT	*Turbine Inlet Temperature*
TOT	*Turbine Outlet Temperature*
CIT	*Compressor Inlet Temperature*

NO	*Oxide of Nitrogen*
CO_2	*Carbon Dioxide*
NPV	*Net Present Value*
CPERT	*Cost Per Emission Reduction Index*
LP	*Linear Programming*
NLP	*Non-linear Programming*
MPP	*Maximum Permissible Power*
LCOE	*Levelized Cost of Energy*
SC	*Super-capacitor*
ESS	*Energy Storage System*
PPL	*Pulsed Power Load*
DC	*Direct Current*
AC	*Alternating Current*
OEM	*Original Equipment Manufacturer*
0-D	*Zero-dimensional*
ICV	*Inter-component Volume*
ICFM	*Iterative Constant Mass Flow*
PI	*Proportional Integral*
PID	*Proportional Integral Derivative*
ADRC	*Active Disturbance Rejection Control*
DBC	*Disturbance-Based Control*
TCES	*Thermochemical Energy Storage*
DNI	*Direct Normal Irradiation*
CS	*Cuckoo Search*
PSO	*Particle Swarm Optimisation*
HIPSO CS	*Hybridising Optimum Improved PSO and CS*
IPSO	*Improved Particle Swarm Optimisation*
FPID	*Fuzzy PID*
MINLP	*Mixed-Integer Nonlinear Programming*
MPC	*Model Predictive Control*
WOA	*whale optimisation algorithm*
GSA	*Gravitational Search Algorithm*
FEP	*Fast Evolutionary Programming*
ACO	*Ant Colony Optimization*
ABC	*Artificial Bee Colony*
SCR	*Silicon-Controlled Rectifier*
GTO	*Gate Turn-Off*
IGCT	*Integrated-Gate Commutated Thyristors*
IGBT	*Insulated Gate Bipolar Transistor*

Si	*Silcom*
SiC	*Silicon Carbide*

1. Introduction

The main objective of work package three (WP3) is to develop innovative methods to enhance aerodynamic, mechanical and electrical aspects of MGTs and utilization of new materials to develop suitable storage systems to enable effective MGT system operation.

Three early-stage researchers (ESRs) are involved in this work package. The section below provides an overview of the ESRs' expected R&D activities within the frame of the project:

WP3: System components innovations and integration with power systems and energy storage

The focus is to investigate innovations in system component design and integration with power systems and energy storage for improved overall performance, increased reliability, reduced cost and flexibility for back-up of intermittent renewables.

ESR10 (CITY) will be concerned with the optimisation of the whole electrical system, consisting of power electronics, high-speed electrical generator and the control system. The aim of the research is to investigate innovative configurations that will significantly reduce the size and cost of the electrical unit, whilst achieving a high overall electrical efficiency (> 95%).

ESR11 (AUTH) will investigate the use of compressed metal foam to enhance the heat transfer efficiency in compact heat exchangers and new CMCs in advanced MGT systems. In addition to developing suitable design and optimisation methods for heat exchangers, this project will explore cost and environmental compatibility of next generation materials for the next generation MGT systems.

ESR12 (UNIGE) will study high temperature energy storage solutions for MGT systems as well as electrochemical storage technologies and the requirements for effective integration with MGTs in applications such as CSP. The output from this ESR will be an optimised management strategy for the MGT-energy storage system, considering both cost and efficiency.

Ultimately, when the innovations are brought together into a single system, the cumulative effect will be to achieve the desired step change in MGT technology.

The tasks, deliverables and milestones of the current periodic reporting are mainly focusing on state-of-the-art studies carried out by the ESRs. However, preliminary results from modelling and experimental work have also been reported in the report.

This report relates to the work provided by ESR10 at CITY which completes the deliverable of the critical review of "Technological advances in electrical and electronic parts and control system".

2. Overview

2.1 Scope

In small-scale power generation, micro gas turbine (MGT) generating systems have outperformed rival technologies (e.g., reciprocating engines). MGT generating system comprises of two main parts: mechanical and electrical. A permanent magnet synchronous machine (PMSM) and power electronics components such as power converters (a rectifier and an inverter or two bidirectional converters) compose up the electrical setup of the microturbine. Microturbine power electronics components are built to satisfy the needs of highly efficient electrical energy production and conversion. In microturbines, the power converter is an important element of the power electronics components. The rapid advancement of power electronics in today's market calls for the development of high-performance power conversion systems capable of providing higher efficiency operating in MGTs. Therefore, identifying some of the advancement that has been done in the power electronics configurations and investigating their applicability in micro gas turbine systems is crucial. New efficient technologies have been deployed in recent years in other applications other than microturbines like electric vehicles and others. Silicon Carbide has largely supplanted silicon as regards the production and the utilization of many devices, such as metal–oxide–semiconductor field-effect transistors (MOSFETs), diodes, Insulated-gate bipolar transistors (IGBTs) and many others. Silicon Carbide (SiC) devices have a low reverse recovery charge, a high carrier saturation velocity that allows for high-frequency operation, and a high breakdown voltage. These devices can function at high temperatures and attain high voltages and currents because of their excellent thermal conductivity and wide bandgap. This work aims to give an overview of the state of the art of the current advancements in power electronics components, a background on the research project and the overall aim and specific objectives.

The basic components of a microturbine generating system can be categorized into two parts: mechanical and electrical.

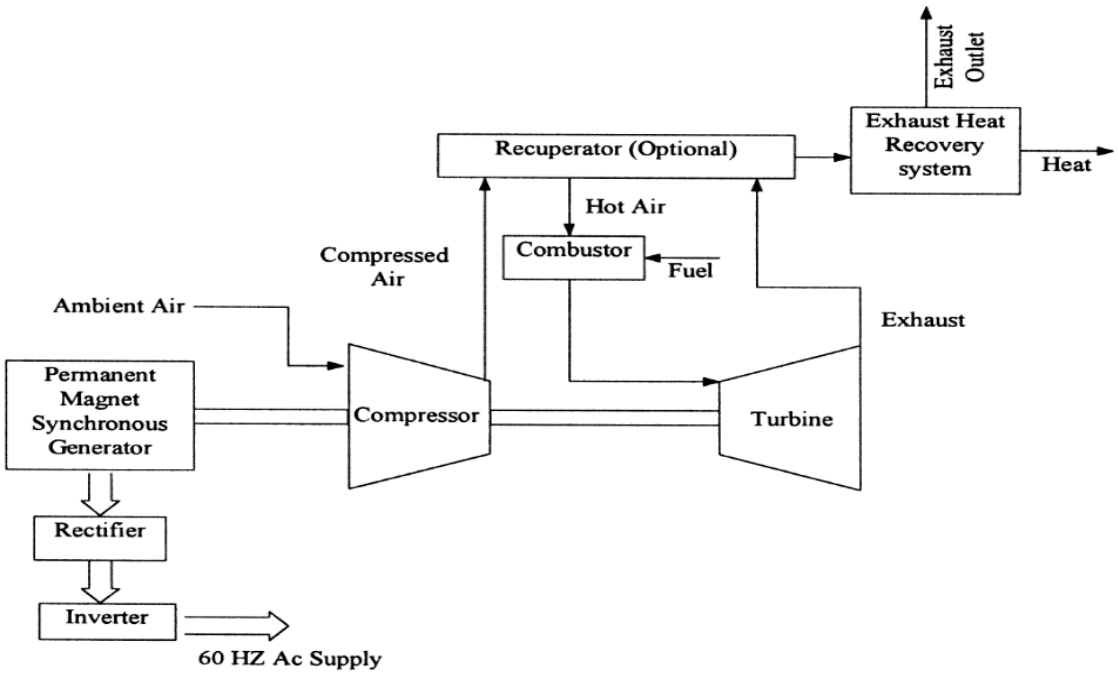

Figure 1: Topology of a Micro Gas Turbine Generation System [4]

As seen in Figure 1: Topology of a Micro Gas Turbine Generation System [4], microturbines' mechanical components generally include an air compressor, combustor, turbine, and recuperator. The electrical part is primarily composed of a permanent magnet synchronous machine (PMSM) and power electronics components such as two bidirectional power converters or a rectifier and an inverter.

The compressor, turbine, and generator are all housed on a single shaft in microturbines. The turbine drives the compressor, which compresses the air, and the generator simultaneously [5]. The compressor of a microturbine pushes air into a recuperator, which recovers heat from the exhaust gas. The heated air is blown into the combustor chamber, where it receives fuel injection. The combusted mixture expands in the combustor chamber, causing the turbine and shaft to rotate and generate electricity through the permanent magnet synchronous machine (PMSM).

2.2 Microturbine Power Conversion Technology

Power electronics components in microturbines are designed to meet the demands of efficient electrical energy generation and conversion. The power converters (rectifiers and inverters) are the prominent parts of the power electronics components in microturbines units. The overall general design of a typical power electronic converter system is shown in Figure 2: Typical Electrical Power Converter Design.

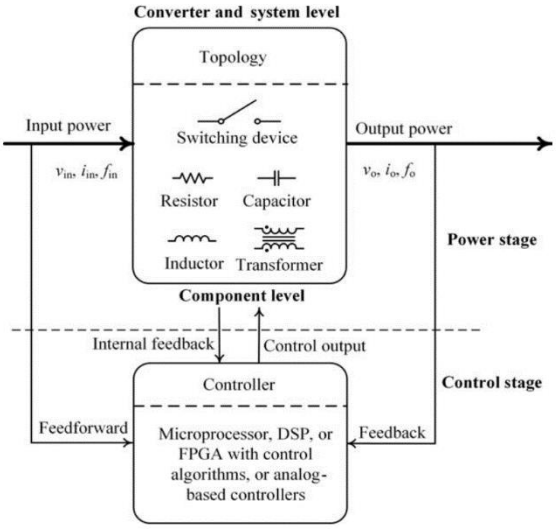

Figure 2: Typical Electrical Power Converter Design [6]

Input voltage v_{in}, input current i_{in}, and input side frequency f_{in} indicate the inputs of the electrical power in the power converter, whereas output voltage v_o, output current I_o, and output side frequency f_o represent the output electrical power. Figure 2: Typical Electrical Power Converter Design [6] depicts the power and control phases, with the top and lower blocks correspondingly labelled. Passive components, such as capacitors, resistors, and inductors, are part of the power stage. Depending on the capabilities of the devices and the application requirements, the switching devices are switched on and off at a frequency ranging from hundreds of Hz to hundreds of MHz. The switching process of such devices or any other process, in either electrical or mechanical parts in the MGT unit, that require controlling is controlled by the controller which is driven by a specific control strategy.

In general, the component-level performance of the MGT units, such as the applied circuit topology of the power electronics components and the utilised control strategy, determines the system-level performance

of the MGT units. As a matter of fact, both power electronics components and their controllers should act appropriately to fulfil supply and demand requirements while also optimising MGT performance [7].

2.3 Power Converters Topologies

The power conversion of a microturbine can be accomplished using either two bidirectional converters or a rectifier and an inverter. The circuits of power converters are composed of semiconductors, mainly diodes. To illustrate more, Figure 3:Three-Phase bidirectional Power Converter Topology shows the structure of a three-phase bidirectional AC-DC converter. The bidirectional AC-DC converter is made up of 6 Insulated-gate bipolar transistor (IGBT) diode switches (S1-S6) that are linked to a three-phase AC voltage source through series filter inductance (Ls) and resistance (Rs).

The bidirectional AC-DC converter has two modes of operation. The first mode is rectifier mode, in which the bidirectional AC-DC converter functions as a front-end rectifier, transferring power from the three-phase AC voltage end to the DC voltage bus. The second mode is inverter mode, in which power flows from the DC voltage bus to the three-phase AC voltage end of the converter, and the converter operates as a voltage source inverter [8].

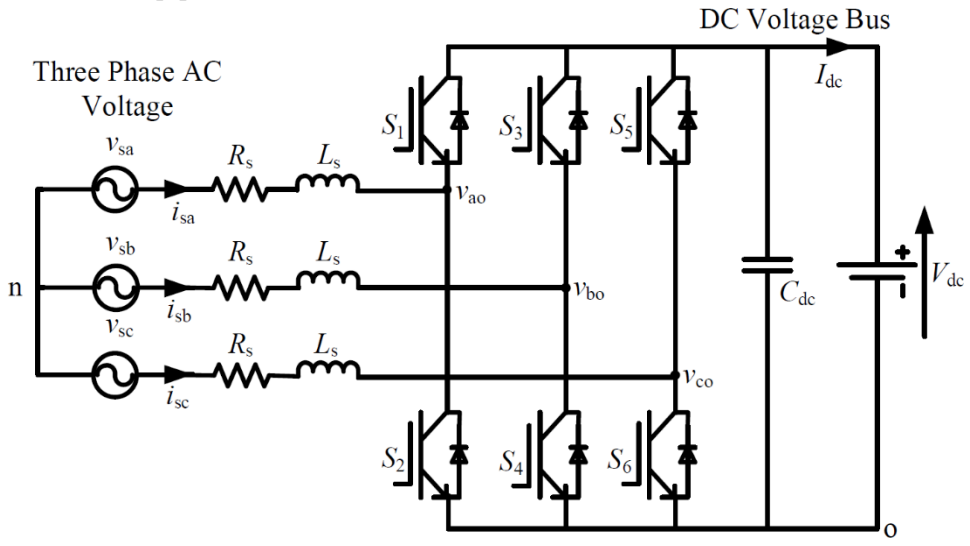

Figure 3:Three-Phase bidirectional Power Converter Topology [8]

2.4 Knowledge Gap

The diodes used in configurating the topology of the power converters in microturbines are based on Silicon (Si) devices such as Si-based IGBTs [9]. In literature, it was not reported any work related to utilising SiC in the power electronics components of microturbines instead of Si. While, in other applications such as electric vehicles and aeroplanes, silicon devices have been replaced by silicon carbide (SiC) devices to configurate their power converters [10], [11]. Why SiC devices are being used instead of Si-based devices is a probable question here. This question can be answered in the next section which addresses the technology of the silicon carbide devices.

2.5 Silicon Carbine Technology

Innovative materials have replaced traditional silicon power devices with the introduction of new efficient power devices. Power devices based on silicon carbide (SiC) might be described as the future of electronics.

These devices are distinguished by their high switching frequency, minimal power losses, and high voltages [12], [13]. They may be used to generate high power and operate at high temperatures because of their excellent thermal conductivity and wide bandgap. These are the reasons why SiC plays an important role in the implementation of new technology applications such as high-efficiency converters [14], [15], power systems for aircraft [16], [17], photovoltaic converters [18], [19], chargers [20], and power supplies for renewable energy systems [21]. SiC devices outperform silicon devices in terms of electrical and thermal properties. They have a high working junction temperature capability, a low on-state resistance, and exceptionally low gate charge and input capacitance, allowing for efficient power converters in a small package.

2.6 Efficiency and Power Losses in Si and SiC Power Converters

Figure 4: Power losses comparison of a rectifier with Si IGBT and SiC MOSFET demonstrates the major forms of losses in a rectifying circuit and the efficiency comparison of the rectifier with Si IGBT and SiC metal–oxide–semiconductor field-effect transistor (MOSFET) at the same voltage level and the same control mode. The efficiency of rectifiers equipped with SiC devices is 2.6 per cent greater than that of rectifiers supplied with Si devices [22]. Further research is required to investigate if employing SiC in the microturbines' power converters may minimize their power losses and improve their electrical efficiency.

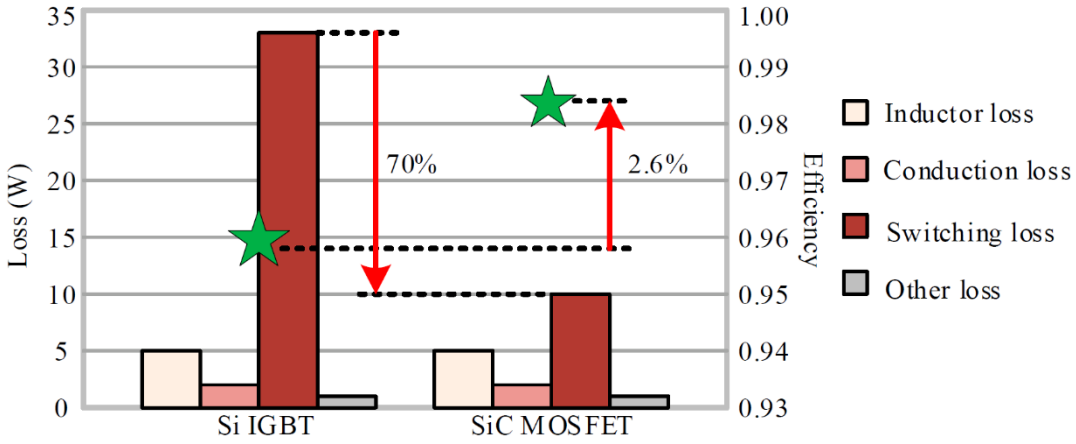

Figure 4: Power losses comparison of a rectifier with Si IGBT and SiC MOSFET [22]

2.7 Power Density in SiC power Converters

Virginia Tech produced a 15 kW 650 V DC/230 V AC three-phase rectifier by replacing all Si devices with SiC JFETs for an aircraft application. The volumetric power density of 6.3 kW/L successfully increased by two kW/L [10]. In microturbines, more specifically, T100, an Ansaldo Energia MGT, takes up more than a third of the setup volume [23].

Figure 5: Ansaldo Energia T100 MGT system for CHP applications [24] may give clearer vision of the generator size compared to the overall size of the microturbine. Further investigations on the potential of reducing the unit size of microturbine’s generator when utilising SiC in their power converters are required.

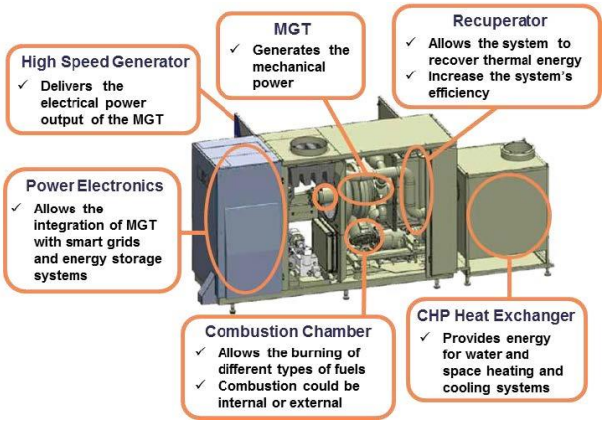

Figure 5: Ansaldo Energia T100 MGT system for CHP applications [24]

2.8 Research Question

The question open for investigation is: What would be the power loss minimization, unit size reduction, and efficiency improvement when substituting Silicon-based power converters in microturbines with Silicon Carbide power converters?

3. Literature Review

3.1 Introduction

This survey aims to perform a critical review of related research. The focus of the literature review in this report can be categorised into two main parts. The first sections go through some of the power electronics advancements that has been done in the power electronics configurations as this work will investigate some of these advancements' applicability in micro gas turbine applications. The focus of the latter sections in this survey is on the impact of different control and operating strategies on the functioning of micro gas turbines. Indeed, both mechanical and power electronics components and their control system must work effectively to meet supply and demand requirements while enhancing the MGT's electrical performance.

3.2 Power Electronics Advancements

Over the last five decades, the power electronics sector has focused on efficiency and power density. Power semiconductor technology, circuit topologies, and control approach significantly impact efficiency and power density. The history of power semiconductors and power electronics are shown in Figure 6: Historical development of power semiconductors and power electronics which has been extracted from an article on the reliability of power electronics [25].

Silicon carbide's high junction temperature, low power losses, and exceptional thermal stability make them an attractive proposition for power converters. Therefore, state of the art in progressions in silicon-carbide power electronic devices will be the centrepiece of this category of literature.

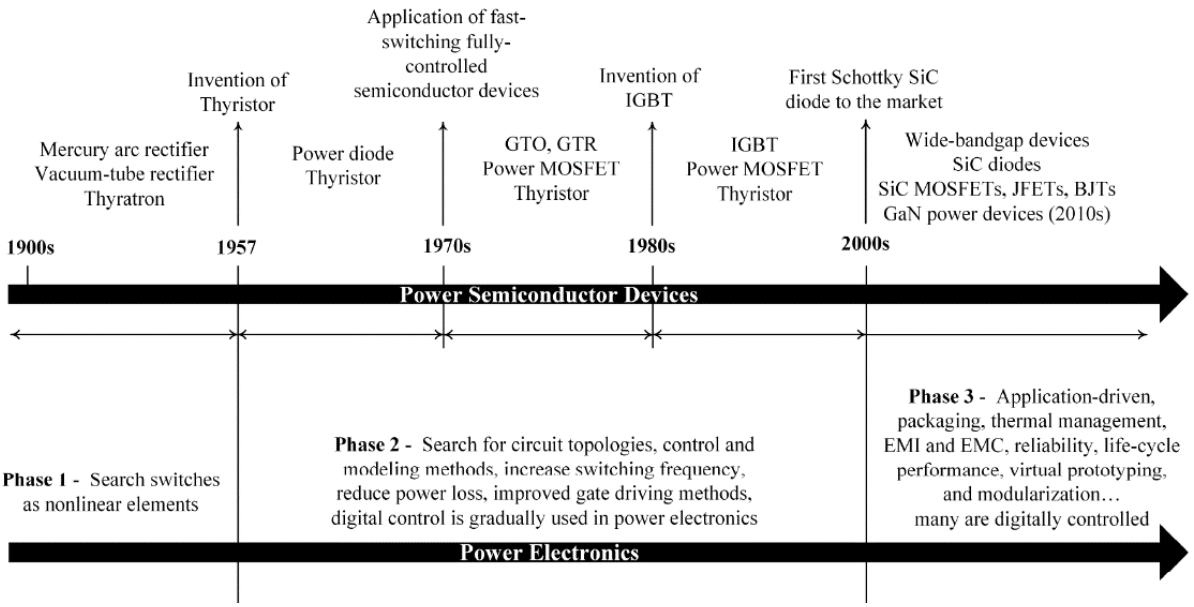

Figure 6: Historical development of power semiconductors and power electronics

3.2.1 Advancement of SiC Devices and their Thermal Capability

In 2001, Infineon developed the first commercial SiC Schottky barrier diode (SiC-SBD), with high blocking voltage, improved thermal stability, and less reverse recovery time. This cleared the door for SiC power devices to be developed in the area of power electronics. Since then, more standalone devices and power modules have steadily appeared [26]. GeneSiC and Micross components offered SiC bipolar junction transistor (BJT) with junction temperatures up to 210 °C till 2014. At the research and development stage, the working junction temperature of SiC-SBD may reach 300 °C, and the performance of SiC positive-negative (P-N) diode has also been proven at 600 °C.

SiC MOSFETs, the most market-oriented SiC devices at this time, feature a high switching speed and a low on-resistance. Palmour et al. from North Carolina State University (NCSU) in the United States created the world's first high-temperature depletion layer N-channel MOSFET in 1987. Brown et al. from GE then built a simulated operational amplifier (OPA) utilising depletion MOSFETs that operate at 300 °C. Purdue University disclosed a SiC digital integrated circuit with a maximum temperature of 350 °C in 2011, although the gate leakage current would rapidly increase as the temperature rises. Commercial SiC MOSFETs can now function at temperatures up to 200 °C [27].

SiC bipolar junction transistors (BJTs), unlike SiC MOSFETs, have high reliability and are suitable for high-temperature operations. GeneSiC's commercialised 1200V SiC BJT that can endure temperatures of up to 210 °C, the highest level on the market. SiC junction field-effect transistors (JFETs) have been developed since the 1990s, with the first commercial SiC JFETs appearing around 2006. Semi South SiC JFETs packed by Micross can withstand up to 200 °C temperatures [28]. Figure 7: Maximum endurance operating temperatures of Si and SiC devices compares the maximum tolerable temperature for commercial power electronic devices at this stage. The data in Figure 7: Maximum endurance operating temperatures of Si and SiC devices are extracted from reference [28].

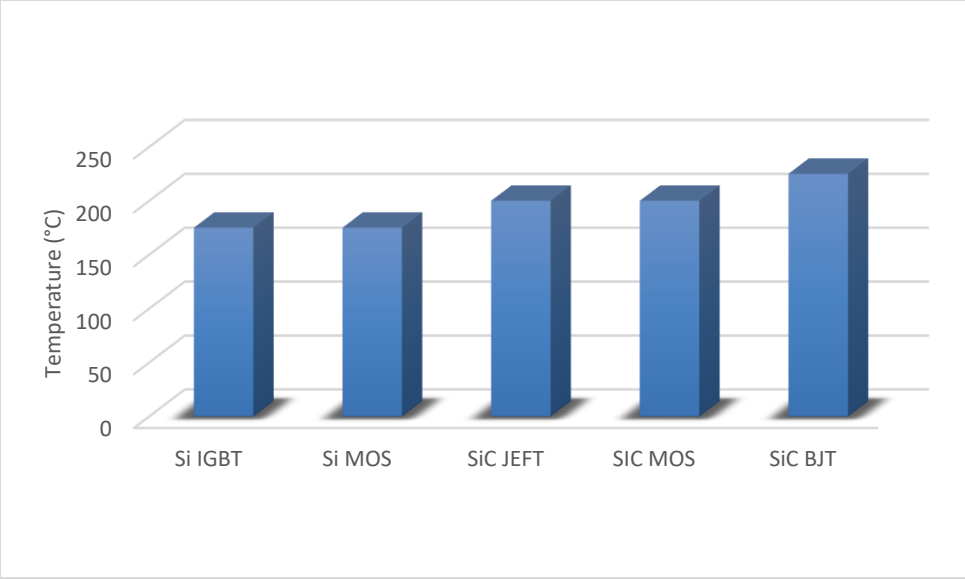

Figure 7: Maximum endurance operating temperatures of Si and SiC devices in market

SiC devices with a large band gap may theoretically allow high voltage and high operating temperatures. However, not all materials' thermal capabilities have attained the same level of technical maturity. Most commercial SiC devices have a maximum working junction temperature of only 210 °C. Tennessee University created a 1.2 kV/100 A SiC JFET power module that operates at 200 °C. Scholars of [29] present a 1.2 kV/60 A SiC MOSFET with improved internal architecture at an operating frequency of 100 kHz and junction temperature of 200 °C. Researchers of [30] present a SiC power module with a junction temperature of 250 °C developed for military hybrid electric vehicle applications. Some discrete devices and integrated circuits have been proven in the laboratory to work at temperatures exceeding 500 °C for a limited period of time [31]. The material and manufacturing of SiC devices are still being researched in order to build high-temperature commercial SiC devices and modules.

3.2.2 Power Losses in SiC Power Converters

In [32], the authors investigate the different behaviour of Si and SiC power MOSFETs in terms of power losses for a DC-DC isolated converter in the automotive field using PowerSIM software simulation tests. The converter operation was simulated using Pulse-width modulation (PWM) control at various switching frequencies up to 600 kHz. It has been noticed that SiC devices perform better in terms of efficiency at the highest frequencies. However, from 20 kHz to 400 kHz, where switching power losses are low, the efficiency measured by SiC devices is lower than the efficiency measured by Si devices because Si MOSFETs' channel resistance is lower than the SiC channel resistance, so SiC conduction power losses are higher than Si ones. Yet, switching power losses grow with frequency: since reverse recovery parameters in SiC devices are lower than those in Si. Switching power losses in SiC devices measured from 400 kHz to 600 kHz are lower than those in Si as shown in Figure 8: Efficiency curves based on SiC and Si. Reproduced from . It has also been found that running at high frequency allows for significant weight and size reductions in filters and transformers.

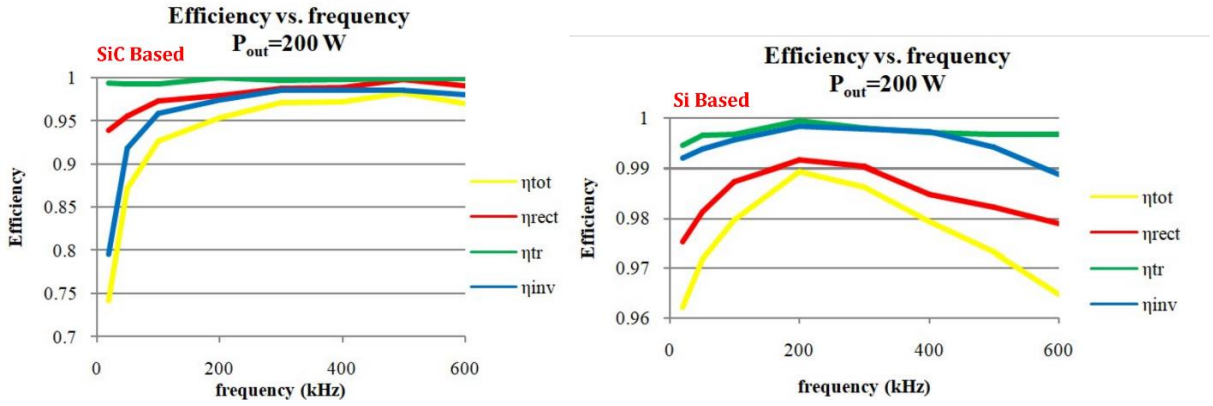

Figure 8: Efficiency curves based on SiC and Si. Reproduced from [32]

3.2.3 Power Density in SiC Power Coverters

For an aeroplane application, Virginia Tech developed a 15 kW 650 V DC/230 V AC three-phase rectifier by replacing all Si devices with SiC JFETs. The 6.3 kW/L volumetric power density was successfully raised by two kW/L [10].

3.2.4 SiC Power Electronics Adoption in Microturbines

The use of silicon carbide devices has been extremely reported for different applications such as electric vehicles, electric aeroplanes, and wind turbines [10], [11], [26], [33]. For instance, Chinese automakers BYD and Toyota have begun using SiC MOSFETs in the traction inverter of their newest Mirai Fuel cell electric vehicles (FCEV) models. Hyundai and Kia also use Hyundai's battery-electric vehicle (BEV) platform to ship cars with SiC-based systems. Several Tier 1 suppliers, like BorgWarner and Denso, are working on SiC-based inverters [11]. For more information about the battery capacity and motor power of such vehicles, please see Figure 9: SiC and Si Adoptions in Electric Vehicles (EV).

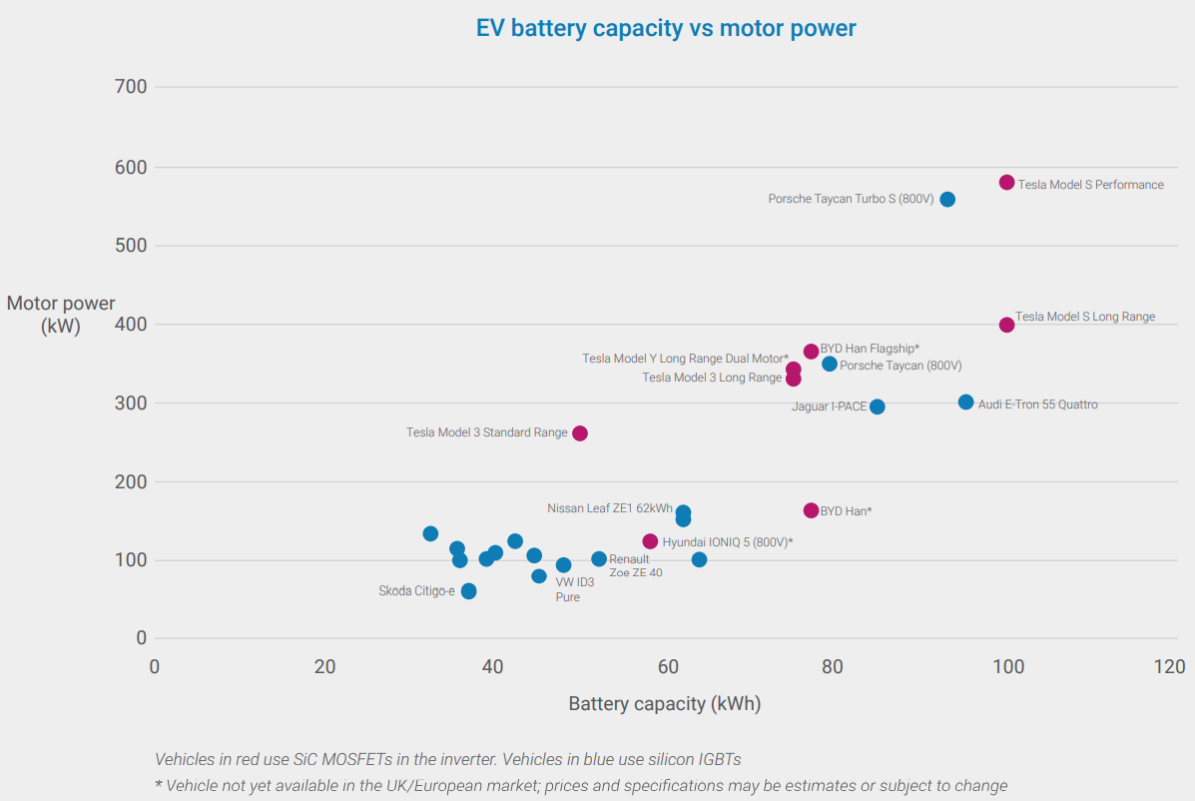

Figure 9: SiC and Si Adoptions in Electric Vehicles (EV) [11]

Although, silicon carbide power devices have received increased attention due to their better properties than silicon-based power devices, the potential of SiC devices has not been reported in the literature for MGT power conversion technology. SiC-based power devices can operate at high voltage, high power, high frequency, and high temperature in a compact size. A SiC-based power converter would have lower losses, greater efficiency, a unit size reduction, fewer passive components, and less vulnerability to excessive ambient heat. SiC-power devices would undoubtedly assist microturbine power converters. More research is needed to establish the system-level advantages of SiC devices in microturbine power converter applications.

3.3 Control Strategies in Micro Gas Turbine Generation Systems

This survey's subsequent sections look at the various control and operational strategies employed in micro gas turbines. In order to meet supply and demand requirements while improving the MGT's electrical performance, mechanical and power electronics components and their control systems must work successfully.

In [34], a voltage controller, speed controller, and active power controller regulate load based on the MGT system's performance. To supply individual resistive-inductive (RL) loads and link to the distributed network, [35] explains dynamic modelling and active power regulation. A complete MGT components and controllers model is presented in [36], along with a unique P-V control approach. Recent research has concentrated on hybrid micro-grids, which combine renewable energy sources with backup generators such as MGTs or diesel generators and Battery Energy Storage (BES). Dynamic modelling, energy management, and control of isolated power production using a microturbine, a tidal turbine, an offshore wind turbine, and lead-acid battery storage are discussed in [37]. As a backup generator, the MGT with battery is employed. It is used in various control approaches to managing the hybrid system's optimum size and

maximum energy extraction from the wind turbine. The photovoltaic (PV) system coupled with the MGT is recommended in [38] for achieving high dependability and continuous power supply with reduced pollution. The performance of a Solid Oxide Fuel Cell (SOFC) connected with four commercially available microturbines at full, and part load has been reported [39]. A rural micro-grid might be powered by a mix of SOFC and microturbines, according to [40]. Biogas serves as the microturbine's fuel, and the inverter acts as a hybrid power system's interface. In any case, the MGT with energy storage system (ESS) may be employed as a standalone distributed generating system to assure power availability at load terminals.

Authors of [41] proposed a system architecture of MGT and supercapacitor (SC) energy storage system (ESS) hybrid power generation to solve the pulsed power load (PPL) problem in the traditional MGT power generation system. There were two types of dual power supply coordination control algorithms presented. One example is the PI-based algorithm for hysteresis control of the DC bus voltage using SC ESS. This approach efficiently suppresses DC bus voltage fluctuation; however, it is a passive response control, and the DC bus voltage continues to fluctuate. The second one is the fast power dynamic response of SC ESS, which can compensate for the low dynamic response of MGT, making the hybrid generation system in an equilibrium state of transient power in real-time. This control method offers the benefits of quick and balanced power distribution, and it was presented based on load conditions, with no effect from the charging process. It was shown that the mixed power supply's two control algorithms are in a real-time instantaneous power equilibrium condition and that the voltage of the DC bus is smooth. The second strategy has a lower DC bus voltage fluctuation and a quicker reaction time. The SC ESS power supply can change the charging power based on the load condition, and it has no effect on MGT throughout the charging process.

PPL is widely seen in distributed generating systems. PPLs such as electromagnetic weapons, electromagnetic launching systems, and free-electron lasers are used in the ship power system explored in [2], [42]. The oilfield drilling microgrid also has a winch load. According to reference [96], PPL produces considerable fluctuations in the frequency of an AC microgrid, huge sags in the voltage of a DC microgrid, and potentially system instability. This has implications for the restricted energy system for self-sufficient or distributed power production [43]–[45]. An effective way to solve the problem of PPL is to add a fast charge and discharge energy storage device to the prime mover generation system to make up for the lack of output power. The supercapacitor is a double-layer energy storage media that does not undergo the Faraday reaction and has properties such as high-power density, extended cycle life, a broad operating temperature range, and so on [46], [47]. As a result, it has found widespread use in distributed power production systems such as fuel cells, electric cars, and wind power generation, where it primarily handles the dynamic response issue of power generation equipment [48], [49]. In [41], because of the introduction of ESS, the issue of PPL has become an ESS control problem. If not managed appropriately, charging of ESS will still lead to substantial voltage and frequency disruptions. The corresponding cooperative control approach is classified into two types. One uses the precise description of output power characteristic of power generation equipment [50], while the other is that there is no need to know the accurate characteristic. Due to easy implementation, control algorithms without precise output power information are widely used to smooth output power of power generation systems, such as PI control, droop control, and so on [51]–[53]. These controls are typically used to generate reference current for capacitance-type ESS charging. Control method selection and controller design decide the difficulties, and maximum power output and smooth output power may be accomplished. Only a few research articles currently integrate SC ESS with MGT power production systems to tackle the PPL issue. To achieve outstanding performance, SC ESS must produce or absorb the appropriate amount of power in the proper time, based on the output power characteristics of the MGT power production system. As a result, the hybrid generating system's power stability may be maintained, and the DC bus voltage remains constant, as suggested in [41].

For further illustration of the meaning of PPL, the change of active power of load is shown in Figure 10: Active Power of Pulse Power Load [41]. It can be observed that the load jumped by 50% in 2 seconds. Also, the unloading procedure is faster where the load is decreased by 100% in 2 seconds. Based on

experiment findings from [45], the results show that the MGT output power change speed is sluggish, and the recovery time is fairly long, falling short of the PPL change speed.

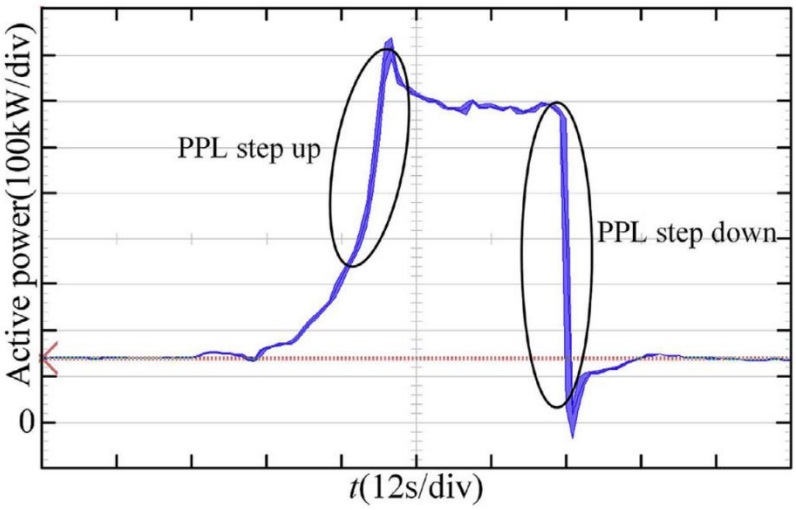

Figure 10: Active Power of Pulse Power Load [41]

3.3.1 Controllers in Steady State and Dynamic Models in MGTs

Model-based controller design strategies may help speed up the development of a cutting-edge controller for micro gas turbines. The dynamic behaviour of MGTs may be described using time-domain models [54] and frequency-domain models [55]. To illustrate the dynamic behaviour of MGTs acquired from identification from experiment data or a nonlinear black-box model, a state-space model [56], [57], a transfer function model [58], and a linear parameter varying model [59] are suggested. These models are simplified, and as a result, some crucial micro gas turbine behaviour may be lost. The accuracy of identification is determined by the collected data and the kind and quantity of the exploration signal fed into the nonlinear black-box model.

Furthermore, artificial intelligence technology proposes surrogate models to define the behaviour of MGTs, such as a neural network model [59]–[61], a NARX model [62], a Markov model [63], and a Wiener model [64]. Surrogate models may also be derived from mass experiment data with a limited sampling time. On the other hand, surrogate models make it difficult to predict unmeasurable MGT characteristics such as safety operating margin and turbine input pressure. Although operational data from an industrial situation may be used to create a sophisticated gas turbine model, such data cannot adequately represent the properties of a micro gas turbine. Without standard documentation data given by the original equipment manufacturer (OEM), the control system upgrade of outdated gas turbines may not perform well and may potentially result in an accident [65]. Many different ways to describe the dynamic behaviour of a gas turbine have been developed [66]–[68]. Because a zero-dimensional (0-D) model can mimic high-quality and quick steady-state and transient-state behaviour, it is frequently utilised in controller design and model-based fault diagnostics [69].

The iterative constant mass flow (ICFM) approach [70], [71] and the inter-component volume (ICV) method [72] are the two basic methods for establishing the 0-D model for gas turbine simulations. Both have been widely researched [73]–[76]. The ICFM approach has two drawbacks. For starters, the model's permissible initial estimated values are computed over several iterations, which is insufficient for real-time condition monitoring and dynamic performance prediction. To be more explicit, the ICFM technique minimises observed errors by modifying the initial estimated values using the Newton – Raphson iterative

method [77]. Second, the ICFM method's premise is inappropriate for analysing the performance of dynamic manoeuvres. Although this is a reasonable assumption for steady-state performance analysis, the fuel flow delivered into the combustor is disregarded when the steady-state conditions are computed. Thus, with the help of a model established by the ICFM method, controllers designed by engineers can satisfy control performance at the steady-state points. Transient-state control performance, on the other hand, may deteriorate. As a result, improving the controller's resilience is an inescapable concern. Controller designers do their utmost to ensure that the gas turbine operates safely under transient state situations to counter the limitations described above. A sliding mode controller, a proportional-integral controller, and a fuzzy controller are among the controllers suggested. Classical proportional-integral (PI) controllers and variable gain PI controllers are commonly used in gas turbines to provide dependable transient-state and steady-state manoeuvre control [78]. A fractional proportional-integral controller, for example, outperforms a traditional proportional-integral controller [78]. The tuning and optimisation of the fractional proportional-integral controller settings, on the other hand, is a difficult problem. The settings of a gain scheduled proportional-integral controller change in response to the operating state of the gas turbine [57]. The gain scheduled proportional-integral controller, on the other hand, is built on an accurate state-space model. The design burden is rather large.

Meanwhile, the fuel flow rate at steady-state operating conditions should be determined ahead of time. At the same time, selecting gain scheduling factors is a difficult process that requires sufficient experience and may be beyond the control engineers' capabilities. The ICV approach is utilised to fulfil a nonlinear nominal model to solve such issues. The initialisation estimated values are validated by steady-state experiment data when the nominal nonlinear model is used for transient state behaviour simulations. In contrast to the ICFM method, the ICV method implies that mass flow imbalances occur during transient-state manoeuvres, which allows it to explain dynamic behaviour more accurately. Furthermore, nitrogen oxides may exceed the relevant limits throughout the gas turbine's life cycle. Because environmental protection is so important, including the nitrogen oxides prediction model into the nominal nonlinear model may guide controller design. The NOx calculation technique is described in detail [79], [80].

3.3.2 Control Strategies in Externally Fired Micro Gas Turbines

The authors of [81] investigated solar-powered micro gas turbines in order to develop optimum control strategies that minimise power output variations and maximise annual generated energy. The three strategies proposed and investigated in this study are power regulation control based on load fluctuation to obtain maximum permitted power for any given value of insolation recuperation control, load fluctuation control based on maximum permitted power for any given value of insolation recuperation control, and power regulation control based on load fluctuation to obtain maximum permitted power.

The recuperation control strategy is based on a hybrid control strategy that combines the previous two tactics while also bypassing the recuperator partially. The efficiency of converting solar energy into electricity, the yearly production of energy, the rated generated power, and other practical aspects all evaluate various techniques. Each of the above control techniques is calculated and compared using a 5-kWe system. According to quantitative and qualitative evaluation, recovery control and combination systems may provide consistent power throughout a wide range of solar irradiation, but at the expense of inferior overall performance, higher cost, and complexity. Using a power control strategy, the quantity of energy generated is maximised. If the generated power of a system is needed to monitor changes in load on the consumer side, it is inadequate.

The writers of [82] investigated the operation and control strategies for a 10 kWe solar MGT system with thermochemical energy storage (TCES). A mathematical model was developed and verified to analyse the system's thermodynamic features under real DNI settings with short- and long-term disruptions. The

impacts of real-time control, such as performance stabilisation and setpoint tracing, are assessed using system dynamics. It was found that when rapidly and drastically variable DNI is predicted, power regulation control strategy may achieve constant speed. It was also shown that power regulation through cascade control might achieve continuous TOT functioning. However, the writers developed a thermodynamic model with some assumptions. For example, the air was regarded as a semi-ideal gas, with the thermodynamic changes in the pipes and connections ignored.

3.4 Response-Demand Control in Micro Gas Turbines

In terms of optimising demand response in MGT systems, the researchers of [83] thoroughly investigates demand response capacity and evaluates possible energy cost reductions. The authors of [84], [85] presented multi-objective models for optimum energy management of grid-connected CHP systems, with reference [85] taking into account real-time pricing through prediction models. Reference [84], on the other hand, is more concerned with carbon emissions. The usefulness of heat storage units for upgrading highly renewable generation-dominated power systems may further increase the economic efficiency of CHP systems [86], [87]. Furthermore, the uncertainty of operational parameters [88] and advanced gas turbine cycles [89] may impact the optimised functioning under real-world operating settings. The CHP optimisation operation is a multi-time scale issue that is dependent on the synchronisation of dispatch instructions at the system level and control systems at the equipment level. References [83]–[87] primarily concentrate on the optimum functioning of the steady-state, although most of them disregard the transient process and crucial equipment features. It is also important to investigate a smaller time-scale optimum issue, concentrating primarily on the control system and regulation.

MGT generating systems, on the other hand, are more flexible than wind turbines and solar systems in that the output power may be considerably more readily adjusted [83]. Following the demand response is therefore a possible operating mode for the MGT-based CHP system, which has been shown in [83] to be more economical than the typical heat-led method. The authors of [90] suggest enhancing the performance of the MGT generating system during the dynamic regulation phase to improve demand response capabilities. The micro gas turbine (MGT) modelling was critical in [90] because it decides if the dynamic reaction of the model matched that of the real CHP system. In order to determine the control settings that combine economy, safety, and speed, an optimisation approach was created. To tackle the optimisation challenge, the improved whale optimisation algorithm (IWOA) with adaptive weights is presented. When compared to pure speed control, it was discovered that the suggested speed and power control is more inexpensive since the steady error is less, and the electricity error during the regulation period may be minimised with appropriate control settings. Furthermore, the suggested IWOA outperforms the original whale optimisation algorithm (WOA) in benchmark function testing and in addressing the parameter optimisation issue in terms of exploitation and exploration. As a result, the suggested control technique in [90] is appropriate for the MGT generating system in terms of improving power demand response capabilities. However, additional research on its application to the CHP system that takes into account more particular thermal system models is required.

3.5 Literature Survey Conclusion

The literature review began with several sections that articulated some of the most recent developments in power electronics components. These innovations have concentrated on silicon-carbide-based components, which are particularly appealing for use in electrical power converters. The main reasons these devices are unique and appealing in power electronics components are their high junction temperature, low power losses, and exceptional thermal stability. The discussion then pivoted more specifically to the advancements in temperature endurance of these devices from their inception to the present. In synopsis, these devices can withstand high temperatures and have excellent thermal stability compared to other silicon devices. Figure 7 depicts the temperature tolerances of some silicon and silicon carbide devices. The differences in power loss between silicon and silicon carbide devices were then introduced in the literature. Silicon carbide

devices have been shown to have reduced power loss than silicon counterparts, especially at very high frequencies, more than 400 kHz, for instance. The discussion then transitioned to another appealing feature of SiC-based devices: the power density they may offer. An example was given for an inverter device developed at Virginia Tech University. The power density of the inverter was increased by 2 kW per litre when all Si devices were replaced with SiC, making the unit smaller for the same power output.

Prior studies in the literature fixated on applications other than microturbines, such as electric vehicles, aircraft, and batteries. This leads to a potential research gap in microturbine power conversion technology. Based on the conducted literature review, there has been no research on attempts at making power electronics components for microturbines based on silicon carbide rather than silicon. More investigation is required to quantify the potential advantages of SiC devices in microturbine power converter applications. Such benefits may include enhanced efficiency and reduced unit size (increased power density).
The other category of the literature went over the control strategies employed in micro gas turbines. Control strategies are critical for the smooth and efficient operation of the microturbine to meet supply and demand requirements while improving the MGT's electrical performance. It was imperative to give a literary overview of microturbines' control and operation strategies since the other part of the work will focus on investigating the capability of the power electronics components to be used as controllers in MGT systems.

References

[1] P. A. Pilavachi, "Mini- and micro-gas turbines for combined heat and power," *Applied Thermal Engineering*, vol. 22, no. 18, pp. 2003–2014, Dec. 2002, doi: 10.1016/S1359-4311(02)00132-1.

[2] R. J. Yinger, "Behavior of Capstone and Honeywell microturbine generators during load changes," Lawrence Berkeley National Lab.(LBNL), Berkeley, CA (United States), 2001.

[3] P. P. Walsh and P. Fletcher, *Gas turbine performance*. John Wiley & Sons, 2004.

[4] Y. Zhan, Z. Cai, Z. Chen, Q. Bao, C. Zhang, and M. Liu, "Control Strategy for Start-Up Process of Micro Gas Turbine Generation Systems," in *2019 22nd International Conference on Electrical Machines and Systems (ICEMS)*, Aug. 2019, pp. 1–4. doi: 10.1109/ICEMS.2019.8922532.

[5] Dieter Deublein and Angelika Steinhauser, "Utilization of Biogas for the Generation of Electric Power and Heat," in *Biogas from Waste and Renewable Resources*, Weinheim, Germany: Wiley-VCH Verlag GmbH & Co. KGaA, 2008, pp. 361–388. doi: 10.1002/9783527621705.ch5f.

[6] H. Wang, F. Blaabjerg, H. S.-H. Chung, and M. Pecht, "Reliability engineering in power electronic converter systems," in *Reliability of Power Electronic Converter Systems*, Institution of Engineering and Technology, 2016, pp. 1–29.

[7] Z. Zhang, R. Pittini, M. A. E. Andersen, and O. C. Thomsena, "A Review and Design of Power Electronics Converters for Fuel Cell Hybrid System Applications," *Energy Procedia*, vol. 20, pp. 301–310, 2012, doi: 10.1016/j.egypro.2012.03.030.

[8] Md. P. Akter, S. Mekhilef, N. M. L. Tan, and H. Akagi, "Model Predictive Control of Bidirectional AC-DC Converter for Energy Storage System," *Journal of Electrical Engineering and Technology*, vol. 10, no. 1, pp. 165–175, Jan. 2015, doi: 10.5370/JEET.2015.10.1.165.

[9] Oak Ridge National Laboratory, "MICROTURBINE POWER CONVERSION TECHNOLOGY REVIEW," Apr. 2003.

[10] D. Zhang *et al.*, "Development of an all SiC high power density three-phase rectifier with interleaving," in *2011 IEEE Energy Conversion Congress and Exposition*, Sep. 2011, pp. 4073–4080. doi: 10.1109/ECCE.2011.6064323.

[11] Compound Semiconductor Applications (CSA) Catapult, Exawatt, and TechWorksHub, "SILICON CARBIDE IN THE UK: ELECTRIC VEHICLES AND BEYOND," Sep. 2021.

[12] W. Zhang, L. Zhang, P. Mao, and Y. Hou, "Characterization of SiC MOSFET switching performance," in *2018 1st Workshop on Wide Bandgap Power Devices and Applications in Asia (WiPDA Asia)*, May 2018, pp. 100–105. doi: 10.1109/WiPDAAsia.2018.8734560.

[13] Z. Meng, Y.-F. Wang, L. Yang, and W. Li, "Analysis of Power Loss and Improved Simulation Method of

a High Frequency Dual-Buck Full-Bridge Inverter," *Energies (Basel)*, vol. 10, no. 3, p. 311, Mar. 2017, doi: 10.3390/en10030311.
[14] W. Zhou and X. Yuan, "Experimental Evaluation of SiC Mosfets in Comparison to Si IGBTs in a Soft-Switching Converter," *IEEE Transactions on Industry Applications*, vol. 56, no. 5, pp. 5108–5118, Sep. 2020, doi: 10.1109/TIA.2020.2999440.
[15] D. Han, J. Noppakunkajorn, and B. Sarlioglu, "Efficiency comparison of SiC and Si-based bidirectional DC-DC converters," in *2013 IEEE Transportation Electrification Conference and Expo (ITEC)*, Jun. 2013, pp. 1–7. doi: 10.1109/ITEC.2013.6574511.
[16] Y. Han, H. Lu, Y. Li, and J. Chai, "Analysis and Suppression of Shaft Voltage in SiC-Based Inverter for Electric Vehicle Applications," *IEEE Transactions on Power Electronics*, vol. 34, no. 7, pp. 6276–6285, Jul. 2019, doi: 10.1109/TPEL.2018.2873079.
[17] D. Han, J. Noppakunkajorn, and B. Sarlioglu, "Comprehensive Efficiency, Weight, and Volume Comparison of SiC- and Si-Based Bidirectional DC–DC Converters for Hybrid Electric Vehicles," *IEEE Transactions on Vehicular Technology*, vol. 63, no. 7, pp. 3001–3010, Sep. 2014, doi: 10.1109/TVT.2014.2323193.
[18] T. Zhao, J. Wang, A. Q. Huang, and A. Agarwal, "Comparisons of SiC MOSFET and Si IGBT Based Motor Drive Systems," in *2007 IEEE Industry Applications Annual Meeting*, Sep. 2007, pp. 331–335. doi: 10.1109/07IAS.2007.51.
[19] F. Shang, A. P. Arribas, and M. Krishnamurthy, "A comprehensive evaluation of SiC devices in traction applications," in *2014 IEEE Transportation Electrification Conference and Expo (ITEC)*, Jun. 2014, pp. 1–5. doi: 10.1109/ITEC.2014.6861777.
[20] G.-J. Su, "Comparison of Si, SiC, and GaN based isolation converters for onboard charger applications," in *2018 IEEE Energy Conversion Congress and Exposition (ECCE)*, 2018, pp. 1233–1239.
[21] D. C. Sheridan, A. Ritenour, R. Kelley, V. Bondarenko, and J. B. Casady, "Advances in SiC VJFETs for renewable and high-efficiency power electronics applications," in *The 2010 International Power Electronics Conference - ECCE ASIA -*, Jun. 2010, pp. 3254–3258. doi: 10.1109/IPEC.2010.5543703.
[22] F. F. Wang and Z. Zhang, "Overview of silicon carbide technology: Device, converter, system, and application," *CPSS Transactions on Power Electronics and Applications*, vol. 1, no. 1, pp. 13–32, 2016.
[23] Turbec AB, "T100 Technical description," 2002.
[24] ETN Global, "Micro Gas Turbine Technology Summary".
[25] H. Wang and F. Blaabjerg, "Power Electronics Reliability: State of the Art and Outlook," *IEEE Journal of Emerging and Selected Topics in Power Electronics*, vol. 9, no. 6, pp. 6476–6493, Dec. 2021, doi: 10.1109/JESTPE.2020.3037161.
[26] Q. Xun, B. Xun, Z. Li, P. Wang, and Z. Cai, "Application of SiC power electronic devices in secondary power source for aircraft," *Renewable and Sustainable Energy Reviews*, vol. 70, pp. 1336–1342, Apr. 2017, doi: 10.1016/j.rser.2016.12.035.
[27] STW100N65G2AG datasheet, "Automotive-Grade Silicon Carbide Power MOSFET 650 V, 100 A, 2 0mW (typ., TJ = 25 C), in a HiP247TM Package," *https://www.st.com/en/power-transistors/sctw100n65g2ag.html*, 2018.
[28] H. Sarnago, O. Lucia, A. Mediano, and J. M. Burdio, "Improved Operation of SiC–BJT-Based Series Resonant Inverter With Optimized Base Drive," *IEEE Transactions on Power Electronics*, vol. 29, no. 10, pp. 5097–5101, Oct. 2014, doi: 10.1109/TPEL.2014.2312216.
[29] Z. Chen, Y. Yao, D. Boroyevich, K. D. T. Ngo, P. Mattavelli, and K. Rajashekara, "A 1200-V, 60-A SiC MOSFET Multichip Phase-Leg Module for High-Temperature, High-Frequency Applications," *IEEE Transactions on Power Electronics*, vol. 29, no. 5, pp. 2307–2320, May 2014, doi: 10.1109/TPEL.2013.2283245.
[30] R. M. Schupbach, B. McPherson, T. McNutt, A. B. Lostetter, J. P. Kajs, and S. G. Castagno, "High Temperature (250 deg C) SiC Power Module for Military Hybrid Electrical Vehicle Applications," ARKANSAS POWER ELECTRONICS INTERNATIONAL INC FAYETTEVILLE AR, 2011.
[31] J. W. Palmour, H.-S. Kong, and R. F. Davis, "Characterization of device parameters in high-temperature metal-oxide-semiconductor field-effect transistors in β-SiC thin films," *J Appl Phys*, vol. 64, no. 4, pp.

2168–2177, 1988.
[32] F. Pellitteri *et al.*, “Power losses comparison between Silicon Carbide and Silicon devices for an isolated DC-DC converter,” in *2021 IEEE 15th International Conference on Compatibility, Power Electronics and Power Engineering (CPE-POWERENG)*, Jul. 2021, pp. 1–6. doi: 10.1109/CPE-POWERENG50821.2021.9501191.
[33] X. Guo, Q. Xun, Z. Li, and S. Du, “Silicon carbide converters and MEMS devices for high-temperature power electronics: A critical review,” *Micromachines (Basel)*, vol. 10, no. 6, p. 406, 2019.
[34] G. Shankar and V. Mukherjee, “Load-following performance analysis of a microturbine for islanded and grid connected operation,” *International Journal of Electrical Power & Energy Systems*, vol. 55, pp. 704–713, Feb. 2014, doi: 10.1016/j.ijepes.2013.10.018.
[35] A. K. Saha, S. Chowdhury, S. P. Chowdhury, and P. A. Crossley, “Modeling and Performance Analysis of a Microturbine as a Distributed Energy Resource,” *IEEE Transactions on Energy Conversion*, vol. 24, no. 2, pp. 529–538, Jun. 2009, doi: 10.1109/TEC.2009.2016123.
[36] S. Grillo, S. Massucco, A. Morini, A. Pitto, and F. Silvestro, “Microturbine Control Modeling to Investigate the Effects of Distributed Generation in Electric Energy Networks,” *IEEE Systems Journal*, vol. 4, no. 3, pp. 303–312, Sep. 2010, doi: 10.1109/JSYST.2010.2059190.
[37] S. M. Mousavi G., “An autonomous hybrid energy system of wind/tidal/microturbine/battery storage,” *International Journal of Electrical Power & Energy Systems*, vol. 43, no. 1, pp. 1144–1154, Dec. 2012, doi: 10.1016/j.ijepes.2012.05.060.
[38] G. Comodi, M. Renzi, L. Cioccolanti, F. Caresana, and L. Pelagalli, “Hybrid system with micro gas turbine and PV (photovoltaic) plant: Guidelines for sizing and management strategies,” *Energy*, vol. 89, pp. 226–235, Sep. 2015, doi: 10.1016/j.energy.2015.07.072.
[39] D. P. Bakalis and A. G. Stamatis, “Incorporating available micro gas turbines and fuel cell: Matching considerations and performance evaluation,” *Applied Energy*, vol. 103, pp. 607–617, Mar. 2013, doi: 10.1016/j.apenergy.2012.10.026.
[40] S. Baudoin, I. Vechiu, H. Camblong, J.-M. Vinassa, and L. Barelli, “Sizing and control of a Solid Oxide Fuel Cell/Gas microTurbine hybrid power system using a unique inverter for rural microgrid integration,” *Applied Energy*, vol. 176, pp. 272–281, Aug. 2016, doi: 10.1016/j.apenergy.2016.05.066.
[41] J. Duan, J. Liu, Q. Xiao, S. Fan, L. Sun, and G. Wang, “Cooperative controls of micro gas turbine and super capacitor hybrid power generation system for pulsed power load,” *Energy*, vol. 169, pp. 1242–1258, Feb. 2019, doi: 10.1016/j.energy.2018.12.004.
[42] X. Feng, K. L. Butler-Purry, and T. Zourntos, “A multi-agent system framework for real-time electric load management in MVAC all-electric ship power systems,” *IEEE Transactions on Power Systems*, vol. 30, no. 3, pp. 1327–1336, 2014.
[43] B. Wu *et al.*, “Design and testing of a 9.5 kWe proton exchange membrane fuel cell–supercapacitor passive hybrid system,” *International Journal of Hydrogen Energy*, vol. 39, no. 15, pp. 7885–7896, May 2014, doi: 10.1016/j.ijhydene.2014.03.083.
[44] F. Bensmaine, O. Bachelier, S. Tnani, G. Champenois, and E. Mouni, “LMI approach of state-feedback controller design for a STATCOM-supercapacitors energy storage system associated with a wind generation,” *Energy Conversion and Management*, vol. 96, pp. 463–472, May 2015, doi: 10.1016/j.enconman.2015.02.059.
[45] Y. Y. Chia, L. H. Lee, N. Shafiabady, and D. Isa, “A load predictive energy management system for supercapacitor-battery hybrid energy storage system in solar application using the Support Vector Machine,” *Applied Energy*, vol. 137, pp. 588–602, Jan. 2015, doi: 10.1016/j.apenergy.2014.09.026.
[46] P. B. Karandikar, D. B. Talange, U. P. Mhaskar, and R. Bansal, “Development, modeling and characterization of aqueous metal oxide based supercapacitor,” *Energy*, vol. 40, no. 1, pp. 131–138, Apr. 2012, doi: 10.1016/j.energy.2012.02.020.
[47] A. Yu, Z. Chen, R. Maric, L. Zhang, J. Zhang, and J. Yan, “Electrochemical supercapacitors for energy storage and delivery: Advanced materials, technologies and applications,” *Applied Energy*, vol. 153, pp. 1–2, Sep. 2015, doi: 10.1016/j.apenergy.2015.05.054.
[48] T. Ma, H. Yang, and L. Lu, “Development of hybrid battery–supercapacitor energy storage for remote area

renewable energy systems," *Applied Energy*, vol. 153, pp. 56–62, Sep. 2015, doi: 10.1016/j.apenergy.2014.12.008.
[49] G. L. Park, A. I. Schäfer, and B. S. Richards, "Renewable energy-powered membrane technology: Supercapacitors for buffering resource fluctuations in a wind-powered membrane system for brackish water desalination," *Renewable Energy*, vol. 50, pp. 126–135, Feb. 2013, doi: 10.1016/j.renene.2012.05.026.
[50] J. Duan, S. Fan, F. Wu, L. Sun, and G. Wang, "Power balance control of micro gas turbine generation system based on supercapacitor energy storage," *Energy*, vol. 119, pp. 442–452, Jan. 2017, doi: 10.1016/j.energy.2016.12.063.
[51] N. Mendis, K. M. Muttaqi, and S. Perera, "Management of Battery-Supercapacitor Hybrid Energy Storage and Synchronous Condenser for Isolated Operation of PMSG Based Variable-Speed Wind Turbine Generating Systems," *IEEE Transactions on Smart Grid*, vol. 5, no. 2, pp. 944–953, Mar. 2014, doi: 10.1109/TSG.2013.2287874.
[52] L. Qu and W. Qiao, "Constant Power Control of DFIG Wind Turbines With Supercapacitor Energy Storage," *IEEE Transactions on Industry Applications*, vol. 47, no. 1, pp. 359–367, Jan. 2011, doi: 10.1109/TIA.2010.2090932.
[53] S. D. G. Jayasinghe and D. M. Vilathgamuwa, "Flying supercapacitors as power smoothing elements in wind generation," *IEEE Transactions on Industrial Electronics*, vol. 60, no. 7, pp. 2909–2918, 2012.
[54] C. Evans, "Testing and modelling aircraft gas turbines: An introduction and overview," 1998.
[55] C. Evans, D. Rees, and D. Hill, "Frequency-domain identification of gas turbine dynamics," *IEEE Transactions on Control Systems Technology*, vol. 6, no. 5, pp. 651–662, 1998, doi: 10.1109/87.709500.
[56] W. Gilbert, D. Henrion, J. Bernussou, and D. Boyer, "Polynomial LPV synthesis applied to turbofan engines," *Control Engineering Practice*, vol. 18, no. 9, pp. 1077–1083, Sep. 2010, doi: 10.1016/j.conengprac.2008.10.019.
[57] M. Pakmehr, N. Fitzgerald, E. M. Feron, J. S. Shamma, and A. Behbahani, "Gain scheduled control of gas turbine engines: Stability and verification," *Journal of engineering for Gas turbines and power*, vol. 136, no. 3, 2014.
[58] D. Yu, H. Zhao, Z. Xu, Y. Sui, and J. Liu, "An approximate non-linear model for aeroengine control," *Proceedings of the Institution of Mechanical Engineers, Part G: Journal of Aerospace Engineering*, vol. 225, no. 12, pp. 1366–1381, Dec. 2011, doi: 10.1177/0954410011400959.
[59] G. I. Pogorelov, G. G. Kulikov, A. I. Abdulnagimov, and B. I. Badamshin, "Application of Neural Network Technology and High-performance Computing for Identification and Real-time Hardware-in-the-loop Simulation of Gas Turbine Engines," *Procedia Engineering*, vol. 176, pp. 402–408, 2017, doi: 10.1016/j.proeng.2017.02.338.
[60] M. Talaat, M. H. Gobran, and M. Wasfi, "A hybrid model of an artificial neural network with thermodynamic model for system diagnosis of electrical power plant gas turbine," *Engineering Applications of Artificial Intelligence*, vol. 68, pp. 222–235, Feb. 2018, doi: 10.1016/j.engappai.2017.10.014.
[61] C. M. Bartolini, F. Caresana, G. Comodi, L. Pelagalli, M. Renzi, and S. Vagni, "Application of artificial neural networks to micro gas turbines," *Energy Conversion and Management*, vol. 52, no. 1, pp. 781–788, Jan. 2011, doi: 10.1016/j.enconman.2010.08.003.
[62] H. Asgari *et al.*, "NARX models for simulation of the start-up operation of a single-shaft gas turbine," *Applied Thermal Engineering*, vol. 93, pp. 368–376, Jan. 2016, doi: 10.1016/j.applthermaleng.2015.09.074.
[63] G. G. Kulikov, V. Yu. Arkov, and A. I. Abdulnagimov, "Markov modelling for energy efficient control of gas turbine power plant," *IFAC Proceedings Volumes*, vol. 43, no. 1, pp. 63–67, 2010, doi: 10.3182/20100329-3-PT-3006.00014.
[64] E. Mohammadi and M. Montazeri-Gh, "A new approach to the gray-box identification of wiener models with the application of gas turbine engine modeling," *Journal of Engineering for Gas Turbines and Power*, vol. 137, no. 7, p. 071202, 2015.
[65] S. Bracco and F. Delfino, "A mathematical model for the dynamic simulation of low size cogeneration gas turbines within smart microgrids," *Energy*, vol. 119, pp. 710–723, Jan. 2017, doi: 10.1016/j.energy.2016.11.033.

[66] B. Song, N. J. Palleroni, L. J. Kerkhof, and M. M. Häggblom, "Characterization of halobenzoate-degrading, denitrifying Azoarcus and Thauera isolates and description of Thauera chlorobenzoica sp. nov.," *International Journal of Systematic and Evolutionary Microbiology*, vol. 51, no. 2, pp. 589–602, Mar. 2001, doi: 10.1099/00207713-51-2-589.
[67] Y. Yu, L. Chen, F. Sun, and C. Wu, "Neural-network based analysis and prediction of a compressor's characteristic performance map," *Applied Energy*, vol. 84, no. 1, pp. 48–55, Jan. 2007, doi: 10.1016/j.apenergy.2006.04.005.
[68] A. Stamatis, K. Mathioudakis, and K. D. Papailiou, "Adaptive simulation of gas turbine performance," 1990.
[69] S. M. Camporeale, B. Fortunato, and M. Mastrovito, "A Modular Code for Real Time Dynamic Simulation of Gas Turbines in Simulink," *Journal of Engineering for Gas Turbines and Power*, vol. 128, no. 3, pp. 506–517, Jul. 2006, doi: 10.1115/1.2132383.
[70] W. I. Rowen, "Simplified Mathematical Representations of Heavy-Duty Gas Turbines," *Journal of Engineering for Power*, vol. 105, no. 4, pp. 865–869, Oct. 1983, doi: 10.1115/1.3227494.
[71] A. J. Fawke, H. I. H. Saravanamuttoo, and M. Holmes, "Experimental Verification of a Digital Computer Simulation Method for Predicting Gas Turbine Dynamic Behaviour," *Proceedings of the Institution of Mechanical Engineers*, vol. 186, no. 1, pp. 323–329, Jun. 1972, doi: 10.1243/PIME_PROC_1972_186_035_02.
[72] B. D. MacIsaac and H. I. H. Saravanamuttoo, "A comparison of analog, digital and hybrid computing techniques for simulation of gas turbine performance," in *Turbo Expo: Power for Land, Sea, and Air*, 1974, vol. 79795, p. V01BT02A044.
[73] C. Wang, Y. G. Li, and B. Y. Yang, "Transient performance simulation of aircraft engine integrated with fuel and control systems," *Applied Thermal Engineering*, vol. 114, pp. 1029–1037, Mar. 2017, doi: 10.1016/j.applthermaleng.2016.12.036.
[74] N. U. Rahman and J. F. Whidborne, "Real-Time Transient Three Spool Turbofan Engine Simulation: A Hybrid Approach," *Journal of Engineering for Gas Turbines and Power*, vol. 131, no. 5, Sep. 2009, doi: 10.1115/1.3079611.
[75] A. Alexiou, I. Roumeliotis, N. Aretakis, A. Tsalavoutas, and K. Mathioudakis, "Modeling Contra-Rotating Turbomachinery Components for Engine Performance Simulations: The Geared Turbofan With Contra-Rotating Core Case," *Journal of Engineering for Gas Turbines and Power*, vol. 134, no. 11, Nov. 2012, doi: 10.1115/1.4007197.
[76] N. U. Rahman and J. F. Whidborne, "A numerical investigation into the effect of engine bleed on performance of a single-spool turbojet engine," *Proceedings of the Institution of Mechanical Engineers, Part G: Journal of Aerospace Engineering*, vol. 222, no. 7, pp. 939–949, Jul. 2008, doi: 10.1243/09544100JAERO389.
[77] Pilidis Pericles, "Digital simulation of gas turbine performance," 1983.
[78] E. Tsoutsanis and N. Meskin, "Performance assessment of classical and fractional controllers for transient operation of gas turbine engines," *IFAC-PapersOnLine*, vol. 51, no. 4, pp. 687–692, 2018, doi: 10.1016/j.ifacol.2018.06.182.
[79] T. S. Pires, M. E. Cruz, M. J. Colaço, and M. A. C. Alves, "Application of nonlinear multivariable model predictive control to transient operation of a gas turbine and NOX emissions reduction," *Energy*, vol. 149, pp. 341–353, Apr. 2018, doi: 10.1016/j.energy.2018.02.042.
[80] N. A. Røkke, J. E. Hustad, and S. Berg, "Pollutant emissions from gas fired turbine engines in offshore practice: Measurements and scaling," in *Turbo Expo: Power for Land, Sea, and Air*, 1993, vol. 78903, p. V03AT15A021.
[81] M. Ghavami, J. Alzaili, and A. I. Sayma, "A Comparative Study of the Control Strategies for Pure Concentrated Solar Power Micro Gas Turbines," Jun. 2017. doi: 10.1115/GT2017-63987.
[82] J. Yang *et al.*, "Thermodynamic modelling and real-time control strategies of solar micro gas turbine system with thermochemical energy storage," *Journal of Cleaner Production*, vol. 304, p. 127010, Jul. 2021, doi: 10.1016/j.jclepro.2021.127010.
[83] M. Houwing, R. R. Negenborn, and B. de Schutter, "Demand Response With Micro-CHP Systems,"

Proceedings of the IEEE, vol. 99, no. 1, pp. 200–213, Jan. 2011, doi: 10.1109/JPROC.2010.2053831.
[84] M. Gitizadeh, S. Farhadi, and S. Safarloo, "Multi-objective energy management of CHP-based microgrid considering demand response programs," in *2014 Smart Grid Conference (SGC)*, Dec. 2014, pp. 1–7. doi: 10.1109/SGC.2014.7090870.
[85] D. Xie, Y. Lu, J. Sun, C. Gu, and J. Yu, "Optimal Operation of Network-Connected Combined Heat and Powers for Customer Profit Maximization," *Energies (Basel)*, vol. 9, no. 6, p. 442, Jun. 2016, doi: 10.3390/en9060442.
[86] P. Vögelin, B. Koch, G. Georges, and K. Boulouchos, "Heuristic approach for the economic optimisation of combined heat and power (CHP) plants: Operating strategy, heat storage and power," *Energy*, vol. 121, pp. 66–77, Feb. 2017, doi: 10.1016/j.energy.2016.12.133.
[87] A. Haupt and K. Müller, "Integration of a LOHC storage into a heat-controlled CHP system," *Energy*, vol. 118, pp. 1123–1130, Jan. 2017, doi: 10.1016/j.energy.2016.10.129.
[88] W. de Paepe, D. Coppitters, S. Abraham, P. Tsirikoglou, G. Ghorbaniasl, and F. Contino, "Robust Operational Optimization of a Typical micro Gas Turbine," *Energy Procedia*, vol. 158, pp. 5795–5803, Feb. 2019, doi: 10.1016/j.egypro.2019.01.549.
[89] W. de Paepe, M. Montero Carrero, S. Bram, F. Contino, and A. Parente, "Waste heat recovery optimization in micro gas turbine applications using advanced humidified gas turbine cycle concepts," *Applied Energy*, vol. 207, pp. 218–229, Dec. 2017, doi: 10.1016/j.apenergy.2017.06.001.
[90] J. Zhu, X. Wang, D. Xie, and C. Gu, "Control Strategy for MGT Generation System Optimized by Improved WOA to Enhance Demand Response Capability," *Energies (Basel)*, vol. 12, no. 16, p. 3101, Aug. 2019, doi: 10.3390/en12163101.
[91] European Commission, "Next Generation of Micro Gas Turbines for High Efficiency, Low Emissions and Fuel Flexibility," *https://cordis.europa.eu/project/id/861079*.